Femtosecond pulses in the focal region of lenses

M. Kempe and W. Rudolph
Department of Physics and Astronomy, The University of New Mexico, Albuquerque, New Mexico 87131
(Received 15 April 1993)

A systematic theoretical and experimental study of focusing femtosecond light pulses by single lenses is presented. By evaluation of the diffraction integral the interplay of spherical and chromatic aberration is shown to determine the temporal as well as the spatial intensity distribution in the focal region of a lens. Conditions are derived under which the effect of spherical aberration dominates. Here a temporally unbroadened, in-focus pulse occurs while the spatial distribution is that expected from an annular lens aperture. If chromatic aberration is the major aberration, the in-focus pulses are considerably broadened. Both effects could clearly be measured with 100-fs pulses using a modified Michelson interferometer. In an intermediate parameter range both chromatic and spherical aberration contribute to the pulse broadening and to the spatial intensity pattern in a given plane in the focal region. From Fresnel diffraction we expect a weak-intensity distribution to precede the in-focus pulse on the axis. Another weak intensity peak is produced by the pulse traveling on axis. By measuring its separation from the main pulse in the marginal focal plane one can estimate the aberration parameters.

PACS number(s): 42.65.Re, 42.79.Bh, 42.25.Fx

I. INTRODUCTION

Many applications of femtosecond light pulses involve focusing by lenses and lens systems, for example, to achieve high on-axis intensities or for beam expansion. Tight focusing producing well-defined wave and pulse fronts is required for such applications as the generation of high field strengths in the focus of terawatt and petawatt pulses [1] and imaging with ultrashort light pulses [2–5]. With available pulse durations in the order of 10 fs [6,7] the optimization of such setups has to be performed not only with respect to the spatial intensity distribution but also with respect to the temporal intensity distribution.

It is well known that chromatic lens aberration leads to a pulse stretching in the focal plane. This results from different arrival times of pulses that pass through the lens at different radial positions as it follows from geometrical optics [8] and was measured in [9]. The effect on the spatial intensity distribution can be explained as the action of a time-dependent aperture. The actual space-time distribution in the focal area is obtained by solving the diffraction integral [10,11]. Using very short pulses the group-velocity dispersion (GVD) in the lens material has to be taken into account in addition. To minimize the GVD effect the pulses can be suitably bias chirped.

Generally, a single lens is not free of spherical aberration. It was shown in [12] that with moderate and strong focusing spherical aberration plays a dominant role for the space-time field distribution in the focal region. Because of spherical aberration, only light passing through a certain lens annulus is brought to a focus in a certain plane. Therefore, the in-focus pulses have the same delay and thus are not broadened if we can neglect GVD.

The aim of our paper is a systematic theoretical and experimental study of the interplay of chromatic and spherical aberration in focusing ultrashort light pulses. In the first part we shall discuss the theoretical approach to obtain the field distribution and derive approximate analytical relations. This is followed by a numerical evaluation of the intensity distribution in the focal region of typical lenses. In the third part we then describe measurements and compare them with the theory.

II. THEORETICAL BACKGROUND

Let us assume a uniform illumination of the lens aperture with a parallel beam. The incident pulse can be thought of as a superposition of monochromatic waves E centered about a midfrequency ω_0. The effect of the lens on a certain spectral component is simply a multiplication with the corresponding amplitude point-spread function (APS) h. Integration over the entire frequency spectrum yields the desired field distribution. The intensity is the corresponding absolute value squared and, in a plane x_1, y_1 a distance z away from the paraxial focal point, is given by

$$I(x_1,y_1,z) \propto \left| \int_{-\infty}^{\infty} d\Delta\omega e^{-j\Delta\omega t} E(\Delta\omega) h(x_1,y_1,z;\Delta\omega) \right|^2 , \tag{1}$$

where $\Delta\omega = \omega - \omega_0$. The problem reduces to finding a suitable representation of the APS. According to the Huygens-Fresnel principle the APS for a circular lens of radius a can be written as

$$h(r_1,z,\Delta\omega) = -\frac{j}{\lambda} \int_0^{2\pi} d\theta \int_0^1 dr \frac{a^2 r}{s f_0 \cos[\arcsin(ar/f_0)]} \times e^{jk(s-f_0)} e^{jk\Phi} e^{-j\Psi} , \tag{2}$$

where f_0 is the paraxial focal length at ω_0, $r_1 = \sqrt{x_1^2 + y_1^2}$ is the radial coordinate, $s = s(\theta, r_1, r)$ is the distance between a point at the reference sphere and the observation point at (r_1, z), $k = \omega/c$, r is a dimensionless radius constant, and θ is the azimuthal angle; see Fig. 1(a). The last two terms in Eq. (2) were introduced to account for aberration. The phase $k\Phi$ describes the deviation of the wave front from a sphere of radius f_0 due to spherical aberration. It is responsible for the fact that to each lens annulus r there corresponds a certain focal length $f(r)$. Considering only the first correction term Φ can be expressed as

$$\Phi = -Ar^4 c/\omega_0 \ , \tag{3}$$

where A is a dimensionless number characterizing the spherical aberration. The quantity Ψ is responsible for the frequency dependence of the optical path length traversed in the lens at radius ar and carries the information about the chromatic aberration. As shown in [10], apart from an unimportant constant factor, Ψ can be written as

$$\Psi(r, \Delta\omega) = \tau r^2 \Delta\omega - \frac{\omega_0}{c}\left(d - \frac{c\tau r^2}{\omega_0 n'}\right) \times (n'/\omega_0 + n''/2)(\Delta\omega)^2 \tag{4}$$

with

$$\tau = \frac{a^2 \omega_0 n'}{2 f_0 (n-1) c} \ , \tag{5}$$

where n, n', n'' are the refractive index and its first and second derivative with respect to ω, respectively, taken at ω_0, and d is the center thickness of the lens. Basically, the first term in Eq. (4) introduces a radius dependent delay $\tau_c(r) = -\tau r^2$ between pulse and phase fronts while the second term is responsible for pulse broadening due to GVD. Note that Eq. (4) is a result of a Taylor expansion of the optical path length up to second order in $\Delta\omega$. Terms of higher order have to be added in the case of strongly dispersive lens materials and/or extremely short pulses (< 10–15 fs in the visible spectral range), which is not to be discussed here.

To illustrate to what extent the pulse and wave fronts just behind the lens are described correctly in Eqs. (3)–(5) we compared them with the results of ray pulse tracing. For two plano-convex BK7 lenses with $f_0 = 100$ mm, $a = 10$ mm, and $d = 1.0$ mm (lens 1) and $f_0 = 200$ mm, $a = 10$ mm, and $d = 0.5$ mm (lens 2), the relative differences are shown in Fig. 2 for $\lambda_0 = 620$ nm. The corresponding parameters characterizing the chromatic and spherical aberration are $\tau = 73$ fs, $A = 28$ and $\tau = 36$ fs, $A = 4$, respectively, where the value for A was determined in the thin-lens approximation [13,12]. Figure 2 suggests that the relative error in the case of moderately focusing lenses is small. As far as pulse fronts are concerned deviations small as compared to the input pulse duration are acceptable, which is satisfied well for both lenses. In contrast, critical phase differences are in the order of π. It is this requirement which limits the applicability of Eqs. (2)–(5). For a better coincidence with the actual phase fronts and to describe systems especially with large A one has to consider higher-order correction terms in addition to the one proportional to r^4 in Eq. (3) or combine ray tracing with diffraction theory directly [14].

For simplicity we shall assume here that the lenses produce phase fronts as given by Eqs. (2)–(5). For the lenses to be described this is a reasonable approximation since the corresponding deviations of the lens surfaces from a perfect sphere amount only to a few wavelengths. Even without additional aberration terms the numerical integration of Eq. (2), i.e., the exact propagation of the wave from the exit plane of the lens to the observation point, involves relative large expense.

As discussed in [15], for $f_0 \gg \lambda_0 \sin^{-2}(\alpha/2)/2$, where $\alpha = \tan^{-1}(a/f_0)$ is the semiaperture angle, the diffrac-

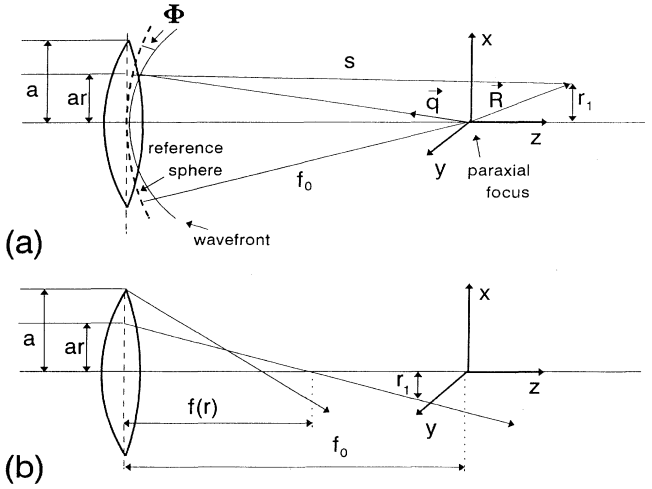

FIG. 1. Lens geometry for (a) the wave optical description and (b) the geometric optical considerations.

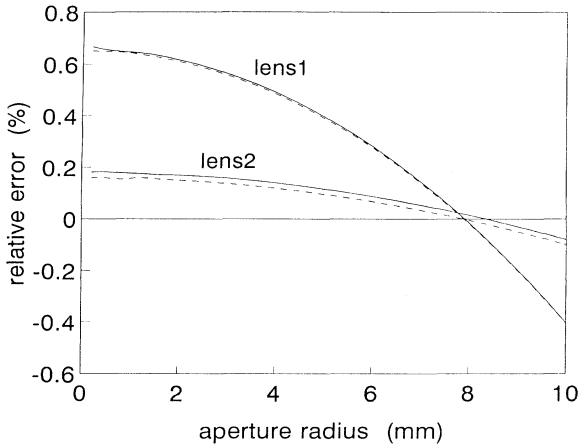

FIG. 2. Relative error of the phase fronts (solid lines) and pulse fronts (dashed lines) as compared with exact ray tracing behind a BK7 lens with $NA = 0.10$ (lens 1) and $NA = 0.05$ (lens 2) vs height ar of the incident rays.

tion problem can be solved in Debye approximation. This is particularly useful for high aperture systems which cannot be described in paraxial approximation. To do this we approximate in Eq. (2) $s - f_0 \approx -\mathbf{q}\cdot\mathbf{R}$ where $\mathbf{q}$ is the unit vector pointing from the paraxial focal point towards the aperture and $\mathbf{R}$ is the position vector to the observation point, see Fig. 1(a). The benefit is that the twofold integration in relation (2) reduces to a single integration over $\mathbf{q}$ within the lens aperture. The aberration terms in Eq. (2) remain unchanged. For a quantitative estimate of the range of validity of the Debye approximation under the conditions of high spherical aberration let us require the difference $(s - f_0) - (-\mathbf{q}\cdot\mathbf{R})$ to be smaller than $\lambda/8$ in the region between paraxial and marginal focal plane. The limiting values were obtained at the focus of the marginal rays and served to estimate a critical aberration parameter. Figure 3 shows the so defined maximum A parameter as function of the numerical aperture (NA) for lenses of different radii. For a particular lens it determines an upper limit for the NA which can still be treated in the frame of this approximation. An example is given as inset in Fig. 3.

In Debye approximation, using the formalism described in [14], the APS (2) can be written as

$$h(r_1, z, \Delta\omega) \propto \int_0^1 dr J_0\left[k_0\left(1+\frac{\Delta\omega}{\omega_0}\right) r_1 \sin(r\alpha)\right] \exp\left[jk_0\left(1+\frac{\Delta\omega}{\omega_0}\right) z\cos(r\alpha)\right] \times \sin(r\alpha)\exp\left[-j\left(1+\frac{\Delta\omega}{\omega_0}\right) Ar^4 - j\Psi(r,\Delta\omega)\right], \tag{6}$$

where $k_0 = \omega_0/c$ and J_0 denotes the Bessel function of first kind and zero order. Here we have approximated the factor $-j/\lambda$ in front of the integral (2) by the constant term $-j/\lambda_0$, with $\lambda_0 = 2\pi c/\omega_0$, which could then be omitted in relation (6) together with other constant factors. It can be shown that the error introduced is negligibly small for pulse durations $>$ 10–15 fs and that this approximation is less severe than the neglect of the third-order dispersion for the temporal and spatial field distribution in the focal region. This is not surprising since the material dispersion appears in a phase term while $-j/\lambda$ is an amplitude term.

It should be mentioned that, if only the field distribution near the paraxial focus is of interest, Eq. (6) approximates the APS from Eq. (2) very well even for large apertures. If, however, the field distribution in the entire focal region is to be discussed the maximum possible numerical apertures become smaller. When the precondition for the paraxial approximation are satisfied the APS can be written as

$$h(r_1, z, \Delta\omega) \propto \int_0^{2\pi} d\theta \int_0^1 dr\, r \exp\left[-jk_0\left(1+\frac{\Delta\omega}{\omega_0}\right)\left\{\frac{arr_1}{f_0}\cos(\theta) + \frac{a^2r^2z}{2f_0^2}\right\}\right] \exp\left[-jAr^4\left(1+\frac{\Delta\omega}{\omega_0}\right) - j\Psi(r,\Delta\omega)\right]. \tag{7}$$

After introducing the common optical coordinates $v = k_0 a r_1/f_0$ and $u = k_0 a^2 z/f_0^2$ we obtain

$$h(v, u, \Delta\omega) \propto \int_0^1 dr\, r\, J_0\left[rv\left(1+\frac{\Delta\omega}{\omega_0}\right)\right] \exp\left[-jur^2/2\left(1+\frac{\Delta\omega}{\omega_0}\right)\right] \exp\left[-jAr^4\left(1+\frac{\Delta\omega}{\omega_0}\right) - j\Psi(r,\Delta\omega)\right]. \tag{8}$$

Since we are not interested in absolute arrival times of the pulse in a certain plane u =const corresponding factors have been neglected.

Before discussing the actual field distribution in the focal region which implies a numerical evaluation of Eq. (6) we want to derive some simple relations that allow us to estimate the effect of chromatic and spherical aberration. The total delay τ_{tot} of a pulse passing through the lens at certain radius r and diffracted to a certain point (v, u) can formally be written as

$$\tau_{\text{tot}} = \tau_c + \tau_s\ , \tag{9}$$

where τ_c was the group delay resulting from chromatic aberration while τ_s is the additional delay caused by spherical aberration. Due to the choice of the time axis this total delay τ_{tot} appears in Eq. (7) in those phase terms which are linear in $\Delta\omega$. Following geometric-optical considerations where we can restrict ourselves to the x-z plane [$\cos(\theta) = 1$] we obtain $r_1 = x_1 \approx \{-z - [f_0 - f(r)]\}ar/f_0$; see Fig. 1(b). The focal length

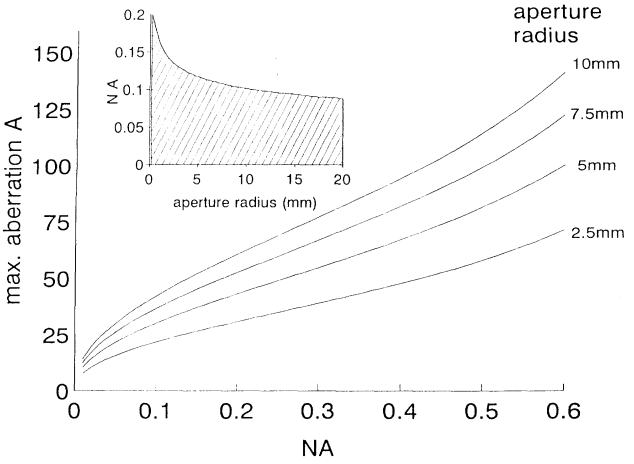

FIG. 3. Maximum amount of spherical aberration which can still be treated in the Debye approximation. The inset gives the range of possible parameters for plano-convex BK7 lenses and $\lambda_0 = 620$ nm.

that corresponds to a lens annulus of radius ar can be written as

$$f(r) = f_0 - \Delta f(r) = f_0 - \frac{4Af_0^2}{k_0 a^2} r^2. \tag{10}$$

With these relations for r_1 and $f(r)$ we obtain for the delay between parts of the pulse front traveling through the lens along the optical axis and at a distance ar and arriving in a certain plane u=const from Eq. (7)

$$\tau_{\mathrm{tot}}(r,u) \approx -\tau r^2 + \frac{3A}{\omega_0} r^4 + \frac{u}{2\omega_0} r^2. \tag{11}$$

Note that their v-values only coincide in the focal plane, i.e., at $u = -k_0 a^2 \Delta f(r)/f_0^2$.

Equations (10) and (11) indicate a complex relationship between spatial and temporal effects. Unlike with monochromatic illumination only those parts of the original wave front interfere the group delay of which is smaller than the pulse length. To illustrate this let us discuss two limiting cases. (i) If the impact of the spherical aberration on the spatial distribution is so small that roughly all rays are in focus in the paraxial focal region of the lens, Eq. (11) describes the temporal stretching of the focused pulse. (ii) If the spherical aberration is large so that rays from different lens annuli have well separated foci, the original pulse duration (strictly speaking, somewhat affected by the GVD of the traversed glass path) will be measured in each focal point.

For a quantitative discussion let us require for case (i) that $\Delta f(0,1) = f_0 - f(r=1)$ is smaller than the focal depth z_d formed by the central part of the beam with radius r_c across which the delay is not larger than the pulse duration τ_p. The radius r_c can be estimated from Eq. (11) by setting $|\tau_{\mathrm{tot}}| = \tau_p$ and $u = 0$. The focal depth produced by an aperture of this radius is $z_d \approx 4\pi f_0^2/(a^2 k_0 r_c^2)$. Using Eq. (10) to express the shift of the focal length, $\Delta f(0,r)$, condition (i) can be written as a condition for the spherical aberration. We obtain

$$A < A_i = \max\left[\pi\,,\, \pi\frac{\tau}{\tau_p}\left(1 - \frac{3\pi}{\omega_0\tau}\right)\right]. \tag{12}$$

One can show that the maximum total delay in the paraxial focus ($u = v = 0$), which can serve as a rough measure for an average pulse duration, is $\tau_{\mathrm{tot}}(r=1) = 3A/\omega_0 - \tau$; cf. Eq. (11). With the maximum aberration according to Eq. (12), A_i, this delay becomes

$$\tau_{\mathrm{tot}}(r=1, u=0) \approx -\tau\left(1 + \frac{9\pi^2}{(\omega_0\tau)(\omega_0\tau_p)} - \frac{3\pi}{\omega_0\tau_p}\right). \tag{13}$$

Obviously, for very short pulses the spherical aberration can modify the pulse duration in the focus in addition to the effect of chromatic aberration (where $\tau_{\mathrm{tot}} \approx -\tau$).

The other limiting case (ii) can be expressed as the condition $|\Delta f(0,r_c)| > z_d$ with r_c defined through $|\tau_{\mathrm{tot}}(r_c)| > \tau_p$. Physically this means that in each plane in the focal region only pulses whose delay is smaller than the pulse duration are in focus. Here the effect of spherical aberration dominates and the in-focus pulses are not broadened. This is expected to occur for

$$A > A_{ii} = \frac{(\tau\omega_0)^2}{9\pi\left[1 + (\omega_0\tau_p)/(3\pi)\right]^2}. \tag{14}$$

To derive this expression we proceeded as above. r_c was determined from Eq. (11) with consideration of (ii) and inserted in Eq. (10). This in combination with (ii) and z_d yields the desired relation for A, cf. Eq. (14). If $\omega_0\tau_p/(3\pi)$ is large compared to 1, we can rewrite relation (14) as $A > \pi(\tau/\tau_p)^2$.

In many practical situations the time-averaged intensity distribution is of interest. With cw light it is convenient to define a so-called circle of least confusion in between paraxial and marginal focal plane at a position $z_l \approx -\frac{3}{4}\Delta f(0,1)$ [16]. An estimate of the temporal width of the focused pulses in this plane can be obtained from Eq. (11) to be

$$\tau_{\mathrm{tot}}(z_l) \approx \tau_s(z_l) + \tau_c(z_l) \approx \frac{1.5A}{\omega_0} r^4 - \tau r^2. \tag{15}$$

With positive A and τ the pulse duration in this plane can expected to be shorter as if one aberration acts alone. It should be mentioned that the optimum focal plane for cw light does not necessarily coincide with the optimum for pulsed illumination.

III. NUMERICAL RESULTS

Using ray tracing and evaluating the corresponding group delay we can easily obtain the pulse fronts in the focal region of a lens at different instants of time. Figure 4 shows several examples for lenses at a wavelength of 620 nm. The time zero was chosen so as to correspond to the arrival of the paraxial rays at their focus. The result for an aspheric lens made from optical grown glass with $f_0 = 8.5$ mm, $a = 4$ mm (referred to as aspheric lens in the following) reflects the effect of chromatic aberration. Here the pulse fronts arrive in the focal plane with a radius-dependent delay $\tau_c = -\tau r^2$ [Fig. 4(a)]. The picture becomes more complex if spherical lenses are used and spherical aberration acts in addition; see Figs. 4(b) and 4(c). In Fig. 4(b) the results for a biconvex BK7 lens with $f_0 = 12.7$ mm, $a = 5.5$ mm, and center thickness $d = 6.68$ mm (in the following called biconvex lens) are depicted. The relevant lens parameters characterizing chromatic and spherical aberration are $\tau = 175$ fs and $A \approx 1835$, respectively. The lens used for Fig. 4(c) is a plano-convex BK7 lens (referred to as plano-convex later on) with $f_0 = 100$ mm, $a = 10$ mm, and center thickness $d = 1.2$ mm, which means $\tau = 73$ fs and $A \approx 28$. With nonzero spherical aberration, not only have pulses passing through different lens annuli different group delays, but they also come to a focus at different positions on the optical axis. In a given plane z=const their delay with respect to on-axis pulses is τ_{tot}. The change of the pulse front even for a moderate value of spherical aberration [Fig. 4(c)] as compared with the aspheric lens is substantial. For this reason the results obtained in [11]

assuming a single lens with $\tau = 4.81$ ps without taking into account spherical aberration are questionable (the A value would be ≈ 5500 for a plano-convex lens).

For the actual space-time distribution of the intensity in the focal region we need to evaluate the diffraction integral (6). Here and in what follows in this section we assume homogeneous illumination at 620 nm with Gaussian-shaped input pulses of duration $\tau_p = 24$ fs so that $E(\Delta\omega) = E_0 \exp[-(T\Delta\omega/2)^2]$ where $T = (2\ln 2)^{-1/2}\tau_p = 20$ fs. For the plano-convex lens the intensity distribution in the paraxial and marginal focal plane is depicted in Fig. 5. Note that a line connecting the maxima would yield the pulse-front distribution as discussed before, however, now in a certain plane rather than at a certain instant of time. The curved pulse front in the paraxial focus and the loop-shaped pulse front in the marginal focus are a result of spherical aberration.

In Fig. 5(b) a small pulse preceding the main pulse can be seen. In the paraxial focal plane, their separation is given by $\Delta t_F \approx -A/\omega_0 - \tau$, which can be derived from an analysis of the phase factors in Eq. (7). A similar pulse was also found in [11] (called forerunner pulse) and explained as result of boundary waves. Our explanation is based on Fresnel diffraction. From an arbitrary on-axis point the lens aperture can be divided into a sequence of Fresnel zones. Note that, neglecting aberrations, as seen from the focal point, the lens aperture contains just one Fresnel zone. The number of Fresnel zones increases if we move away from the focus. If the temporal delay of pulses passing the lens through neighboring Fresnel zones caused by chromatic aberration is smaller than the pulse duration their contribution to the on-axis intensity is approximately zero due to destructive interference. What is generally left is a contribution from an annulus at the lens rim which lacks a counterpart for destructive interference. Hence it gives rise to a pulse appearing at a time when the pulses from the aperture edge pass the axis. As we move towards (or away from) the lens we continuously change the number of Fresnel zones and the size of the "left-over" annulus. This suggests a periodic behavior of the amplitude of the prepulse which is also expected if the aperture radius is changed. Detailed numerical calculations (not shown here) reveal this behavior and support this discussion. With spherical aberration the same discussion holds except that there is no on-axis position for which the lens aperture seems to contain only on Fresnel zone. This reflects the fact that there is no single focus. The occurrence of a prepulse in the paraxial focal plane for the particular lens chosen here is a direct consequence of spherical aberration.

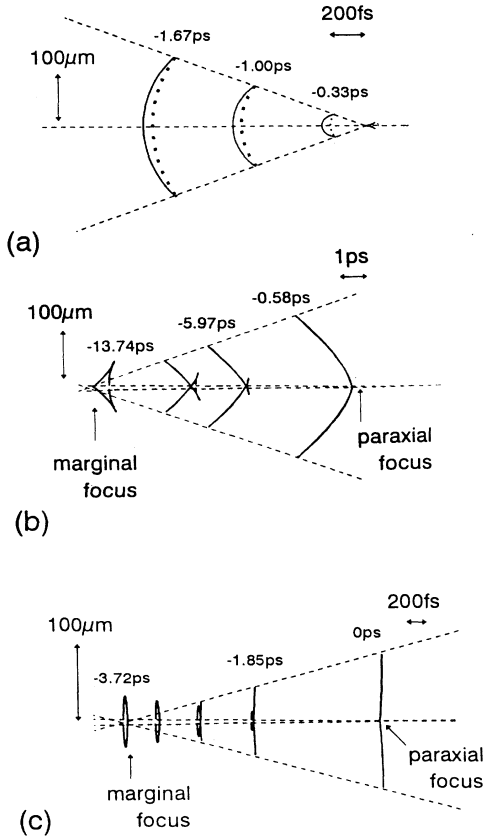

FIG. 4. Pulse fronts (solid lines) in the focal region of different lenses obtained from pulse ray tracing. The dashed lines indicate the propagation of the marginal and paraxial rays. The dotted line in (a) represents the phase fronts. (a) aspheric lens with $\tau = 130$ fs, (b) biconvex lens with $\tau = 175$ fs and $A = 1835$, and (c) plano-convex lens with $\tau = 73$ fs and $A = 28$. The detailed lens parameters are given in the text.

In general an on-axis observer in the focal region "sees" different intensity peaks passing by—($p1$) a pulse corresponding to light which is in focus, ($p2$) a (weak) pulse that travels along the optic axis, and ($p3$) the (weak) "Fresnel" pulse. Their relative timing depends on the position z of the observation plane and the aberration parameters. The temporal separation Δt_F of an in-focus pulse and the "Fresnel" pulse is given by $\Delta t_F(r) \approx -A/\omega_0(1-r^2)^2 - \tau(1-r^2)$. In the marginal focal plane ($p1$) and ($p3$) coincide while in the paraxial focal plane ($p1$) and ($p2$) are equivalent. The remaining two maxima in these planes can be clearly seen in Fig. 5.

From a practical point of view it is interesting to investigate the temporal behavior of the pulse power, i.e., the intensity integrated over its spatial distribution in a certain plane in the focal region. To characterize the spatial distribution it is convenient to analyze the pulse energy contained in a circle of radius r_1. Corresponding numerical results for the plano-convex lens are shown in Fig. 6. The temporal width of the pulse power, see Fig. 6(a), can be well approximated with the analytical formula (11) for τ_{tot} with $r = 1$. The effective pulse duration is smallest in the paraxial focus. As far as focusing is concerned, a plane in between marginal and paraxial focus yields the narrowest, integral spot size. To illustrate this we show the energy distribution in the plane of least confusion known from focusing of cw-light; see Fig. 6(b). It should be noted that this plane is not necessarily the optimum one for ultrashort pulse focusing. With a lens that satisfies condition (ii), however, the intensity distribution near the optical axis closely resembles that obtained with cw

light. In contrast, for a lens of small A but $\tau > \tau_p$ the focal spot becomes broader as compared with cw illumination [10].

As outlined in Sec. II if condition (ii) and relation (14) are satisfied, the focal regions of pulses whose time delay is longer than the pulse duration do not overlap. Therefore in an experiment in which nonlinear light-matter interaction favors the high in-focus intensities, the relevant pulse duration is the original one (if GVD can be neglected). This is despite the fact that the total delay τ_{tot} can exceed τ_p several times. As a consequence, if such a lens is used in an autocorrelator to focus onto the second harmonic generation crystal, the undisturbed pulse duration can be measured [12]. In the same setup with an aspheric lens one would measure τ_c which can be much larger than τ_p. For illustration we calculated the autocorrelation width obtained with the plano-convex lens with $A \approx A_{ii}$ and $\tau = 73$ fs and compared it with that from a lens with equal aperture but with $A = 4 < A_{ii}$ and $\tau = 36$ fs ($f_0 = 200$ mm). While the former does not

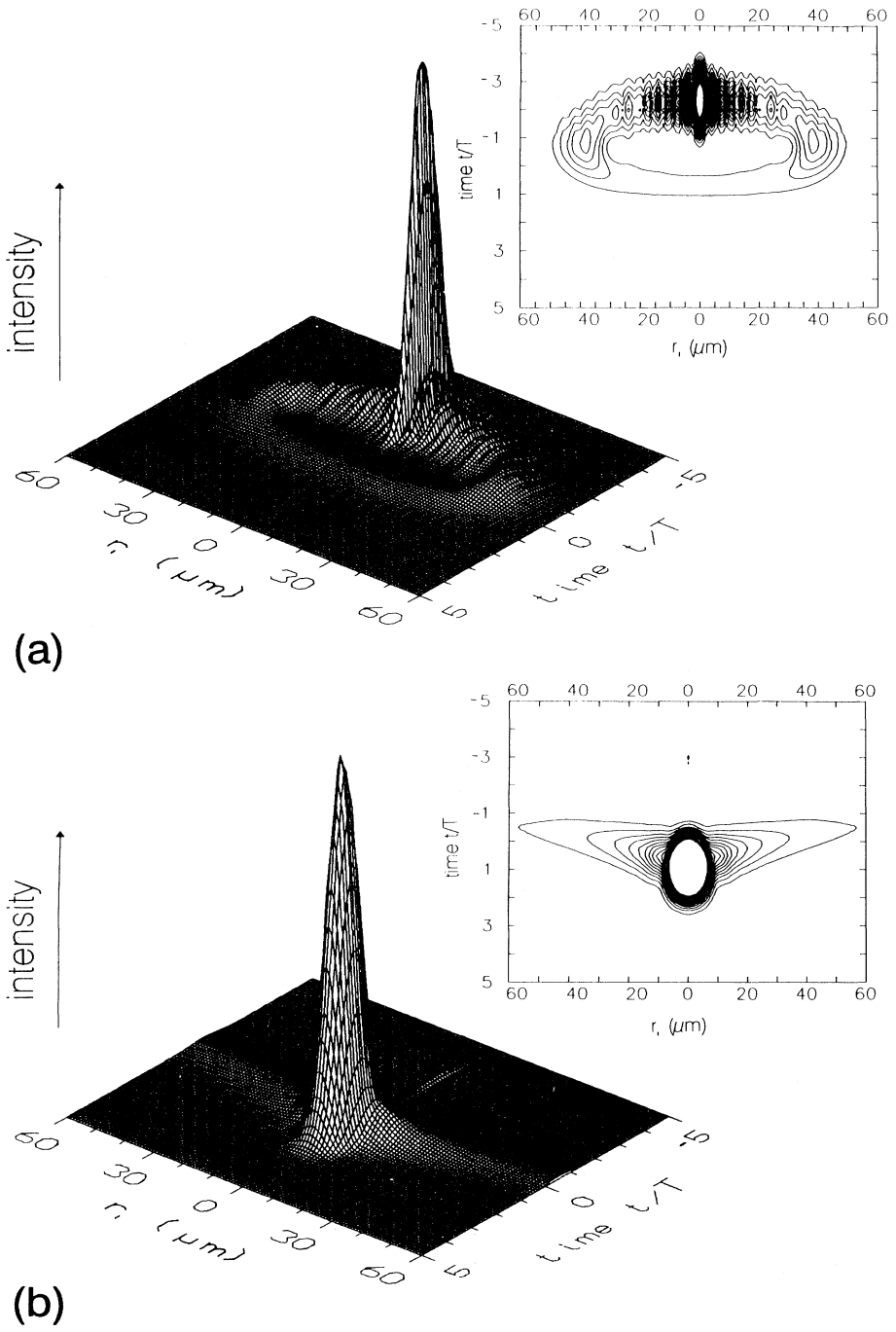

FIG. 5. Space-time distribution of the intensity (a) in the marginal and (b) the paraxial focal plane of the plano-convex lens. Note the time origin is chosen arbitrarily. For the lens parameters we refer to Fig. 4 and the text. The insets show a topographic view of the intensity distribution.

introduce a broadening the use of the second lens results in a broadening factor of 1.25, although its τ/τ_p value is two times smaller.

IV. EXPERIMENTAL RESULTS AND COMPARISON WITH THEORY

For the measurement of the phase and pulse-front distortions introduced by a lens with chromatic and spherical aberration we used the modified Michelson interferometer depicted in Fig. 7.

The beam of a femtosecond dye laser (100 fs, 620 nm) is expanded and then divided by a beam splitter. One arm of the interferometer contains the lens to be characterized in front of a plane mirror M_1. The length of the reference arm can be adjusted by the position of mirror M_2. By translating the lens, light passing through it at different radial positions r can be focused onto M_1.

Provided the reference arm has proper length an interference pattern can be observed at the output of the interferometer. Since the visibility of an interference pattern requires the phase fronts from the two arms of the interferometer to be (almost) parallel, only light which is in focus at M_1 or/and which travels exactly along the optical axis through the lens can contribute. Thus the radius of the fringe pattern is a direct measure of the radius of the annulus of light which is in focus on mirror M_1 for a certain value of Δf. The second requirement is that the group delay over the observed annulus is less than a pulse duration. Corresponding measurements are shown in Fig. 8 for the biconvex BK7 lens described in Sec. III. The dashed line is a theoretical curve obtained

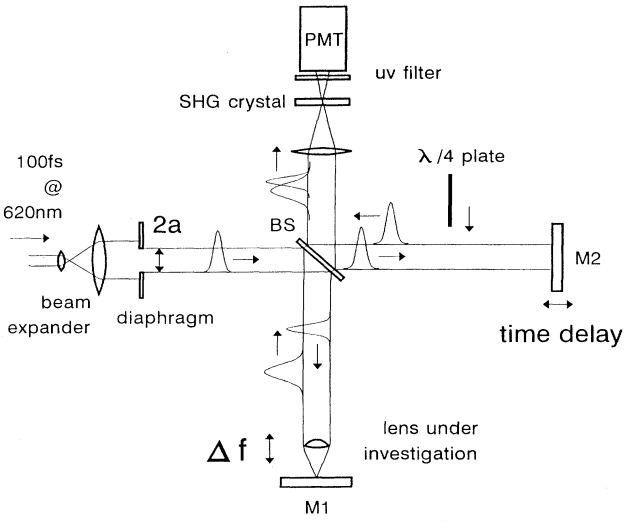

FIG. 7. Experimental setup to measure the effect of lenses on the focusing of femtosecond light pulses.

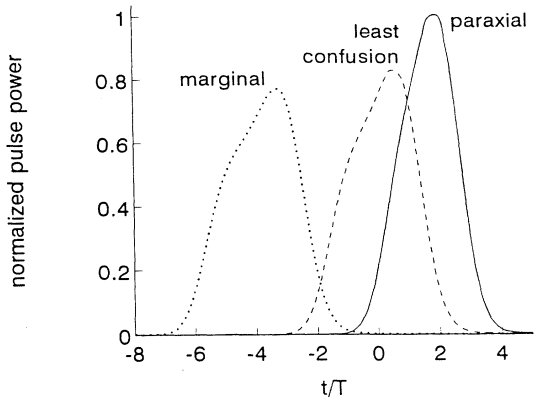

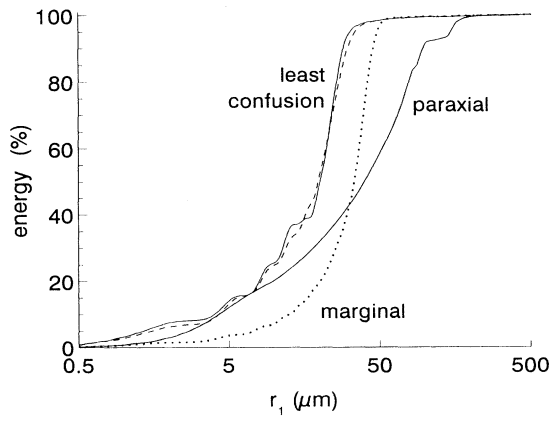

FIG. 6. (a) Pulse power and (b) pulse energy contained in a circle of radius r_1 in different planes in the focal region of the plano-convex lens (paraxial plane, solid line; plane of least confusion, dashed line, marginal plane, dotted line). In (b) the pulse energy in the plane of least confusion with cw illumination is shown for comparison (solid line).

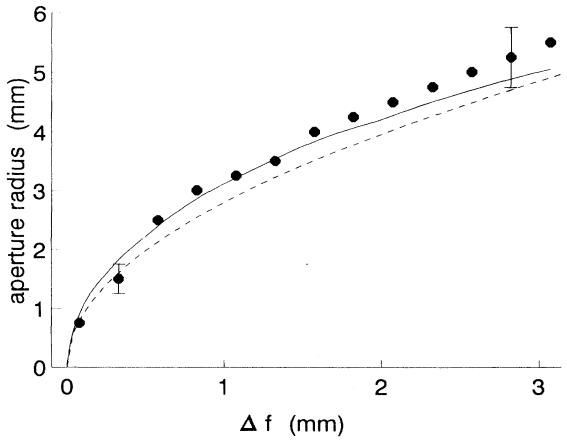

FIG. 8. Spherical aberration of the biconvex lens [•, measurement; solid line, ray tracing; dashed line, result according to Eq. (10) with $A = 1835$].

from Eq. (10) with $A = 1835$. For comparison the result of exact ray tracing is also shown.

Information on the group delay and pulse duration is obtained by cross correlating the pulses from the two interferometer arms in a nonlinear crystal for second harmonic generation. Here the phase matching condition imposes a selection of almost parallel wave fronts. Figure 9 shows the delay of mirror M_2 at which the maximum cross correlation signal occurs versus the position of the lens.

The zero was chosen for the paraxial rays being in focus. The dashed line corresponds to the delay parameter according to Eq. (11) and the solid line was obtained with exact ray pulse tracing. At a given position Δf the measured delay is the delay between pulses passing through the lens center and those passing through an annulus of radius ar in the corresponding focal plane. Note that although the lens parameters are beyond the validity range of our analytical formulas, the results for the total delay are in qualitative agreement with the measurements. It should also be mentioned here that we actually characterize not the focusing by a single lens but the effect of a telescope of magnification one consisting of two equivalent lenses. It is easy to show, however, that the radius-dependent phase and pulse delays simply double their values in this case.

The normalized full width at half maximum (FWHM) of the cross correlations is depicted in Fig. 10, which indicates that there is (almost) no pulse broadening within the experimental error.

This is not surprising because with the lens parameters $A \approx 1800$ and $\tau_c \approx 175$ fs we satisfy condition (14). For comparison the FWHM of the cross correlation obtained with the aspheric lens is shown too. Here relation (12) is valid and the expected pulse duration is roughly $\tau_p' \approx \tau_c$. In fact, the measured pulse duration (assuming Gaussian pulses) was 250 fs compared to the calculated value of

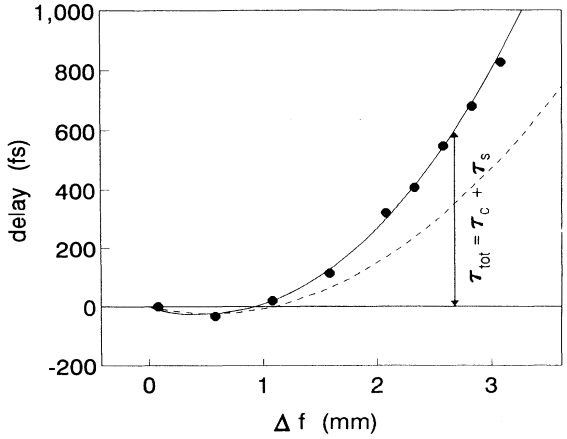

FIG. 9. Position of the cross correlation peak vs distance of M_1 from the paraxial focus [• measurement; solid line, ray tracing; dashed line, result according to Eq. (11)].

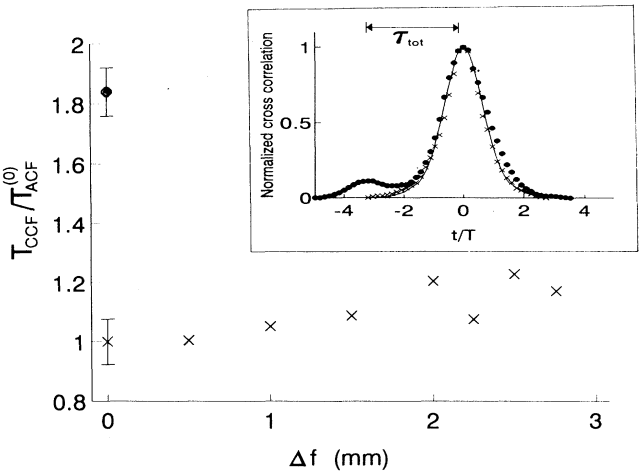

FIG. 10. FWHM of the cross correlation normalized to the FWHM of the autocorrelation of the input pulses obtained with the biconvex BK7 lens (×) and the aspheric lens (•). The inset shows the measured cross correlation in the paraxial plane (×) and at $\Delta f = 2.75$ mm (•) for the biconvex lens. The solid line represents the autocorrelation of the input pulses.

$\tau_p' \approx 2\tau_c \approx 265$ fs (note the factor 2 results from the double passage through the lens).

Typical cross correlation traces for the spherical lens are depicted as inset in Fig. 10 for $\Delta f = 2.75$ mm ($ar = 5.25$ mm) and $\Delta f = 0$. A small satellite preceding the main peak can be clearly seen in the curve with $\Delta f = 2.75$ mm. It represents the cross correlation between reference pulse and the pulse traveling along the optical axis through the lens. The temporal separation between the two correlation peaks thus equals τ_{tot} as expected from the discussion above.

V. CONCLUSIONS

The focusing of femtosecond light pulses with single lenses was studied theoretically and experimentally. The unavoidable interplay of chromatic and spherical aberration determines the space-time characteristics of the intensity distribution in the focal region. Conditions are derived under which spherical aberration dominates. Here a temporally unbroadened, in-focus pulse occurs while the spatial distribution is that expected from an annular lens aperture. If chromatic aberration is the major aberration the in-focus pulses are considerably broadened. Both effects could clearly be observed with 100-fs pulses. In an intermediate parameter range both chromatic and spherical aberration contribute to the pulse broadening and to the spatial intensity pattern in a given plane in the focal region. From Fresnel diffraction we expect a weak-intensity distribution to precede the in-focus pulse on the axis. Another weak-intensity peak is produced by the pulse traveling on-axis. By measuring

its separation from the main pulse, for example, in the marginal focal plane one can estimate the aberration parameters. If two lenses are used for beam expansion the pulse front behavior, in particular the radius-dependent delay, can simply be estimated adding the corresponding values for $\tau_{\mathrm{tot}}(r)$ of the two lenses.

ACKNOWLEDGMENTS

We thank Dr. J.-C. Diels for essential support. This work was supported in part by the Sandia University Research Program. M. K. acknowledges support from the Daimler-Benz Foundation, Ladenburg, Germany.

[1] Y. Beaudoin, C. Y. Chien, J. S. Coe, J. L. Tapie, and G. Mourou, Opt. Lett. **17**, 865 (1992).
[2] C. Yan and J. C. Diels, Appl. Opt. **31**, 6869 (1992).
[3] K. M. Yoo, Q. Xing, and R. R. Alfano, Opt. Lett. **16**, 1019 (1991).
[4] H. Chen, Y. Chen, D. Dilworth, E. Leith, J. Lopez, and J. Valdmanis, Opt. Lett. **16**, 487 (1991).
[5] M. Kempe and W. Rudolph, J. Opt. Soc. Am. A **10**, 240 (1993).
[6] R. L. Fork, C. H. Brito-Cruz, P. C. Becker, and C. V. Shank, Opt. Lett. **12**, 483 (1987).
[7] P. F. Curley, Ch. Spielmann, T. Brabec, F. Krausz, E. Wintner, and A. J. Schmidt, Opt. Lett. **18**, 54 (1993); M. T. Asaki, C. P. Huang, D. Garvey, J. Zhou, H. C. Kapteyn, and M. M. Murnane, *ibid.* **18**, 977 (1993).
[8] Z. Bor, J. Mod. Opt. **35**, 1907 (1988).
[9] Z. Bor, Z. Gogolak, and G. Szabo, Opt. Lett. **14**, 862 (1989).
[10] M. Kempe, U. Stamm, B. Wilhelmi, and W. Rudolph, J. Opt. Soc. Am. B **9**, 1158 (1992).
[11] Z. Bor and Z. L. Horvath, Opt. Commun. **94**, 249 (1992).
[12] M. Kempe and W. Rudolph, Opt. Lett. **18**, 137 (1993).
[13] M. Born and E. Wolf, *Principles of Optics* (Pergamon, London, 1989).
[14] J. J. Stamnes, *Waves in Focal Regions* (Hilger, Bristol, 1986).
[15] E. Wolf and Y. Li, Opt. Commun. **39**, 205 (1981).
[16] W. T. Welford, *Aberrations in Optical Systems* (Hilger, Bristol, 1986).